Collective Resonance in Large Free Potassium Cluster Ions

C. Bréchignac, Ph. Cahuzac, N. Kebaïli, J. Leygnier, and A. Sarfati

Laboratoire Aimé Cotton, Centre National de la Recherche Scientifique, Batiment 505 Campus d'Orsay, 91405 Orsay CEDEX, France

(Received 22 October 1991)

The absorption cross-section profile of large charged clusters is measured by a new procedure based on multistep photoabsorption experiments. Comparison is done with the predictions of classical and quantum treatments. In light of these results, size trends in the optical properties of alkali clusters are discussed.

PACS numbers: 78.20.−e, 36.40.+d

Recent measurements of the visible photoabsorption spectra of small alkali-metal clusters [1–6] have been done to probe the electronic structure of those particles. Theoretical investigations [7–12] have followed the same progression as experimental studies did. One interesting question is how many atoms are required to make a cluster exhibiting collective effects. Two size domains may be distinguished: the very small sizes, smaller than the heptamer, for which *ab initio* molecular orbital calculations including electron configuration interaction completely reproduce the absorption features [11], and the larger sizes, for which the valence electrons are numerous enough to induce collective effects such as the well-known surface plasma resonance. For this last case the random phase approximation (RPA) in the local density approximation (LDA) [12] is a common theoretical baseline which can be used to interpret the experimental data. Up to now experiments have been performed on free clusters containing less than 40 atoms [1–3]. This size domain is too limited to probe the behavior toward the bulk and to correctly test the hypothesis of RPA-LDA treatments.

In this Letter we present the collective resonance cross section of large potassium cluster ions K_n^+ containing 500 and 900 atoms. For such sizes the single-photon depletion technique used for photoabsorption measurements for small sizes is hopeless [13]. So we developed a new procedure based on multistep photon absorption followed by evaporation. Our results provide evidence of the plasma resonance energy of potassium cluster blueshifted as cluster size increases and converging very slowly toward the bulk value. Such an evolution is discussed in light of the different theoretical models.

The experimental procedure is based on the concept of photoinduced evaporation [14]. Adiabatic expansion of potassium generates a cluster distribution centered around 600-atom clusters. The distribution is photoionized by a pulsed UV laser . The accelerated cluster ion bunches first enter a field-free tube where they spatially resolve into separated ion packets within a mass resolution larger than 200. After size selection, a given cluster ion bunch enters a decelerating-accelerating region where it interacts with a second pulsed laser. The ion products from photointeraction are mass analyzed by a second time-of-flight spectrometer.

It is well known that for metal clusters the electronic excitation resulting from the visible photon absorption relaxes very rapidly among the numerous vibrational modes providing unimolecular evaporative cooling in the ground state [15]. For small cluster sizes the detection of the fragmentation produced from unimolecular evaporation after single-photon absorption allows the measurement of absorption cross section as has been already done for $n < 20$ [2]. However, it has been noted that, at constant excitation energy, the unimolecular dissociation rate decreases with increasing cluster size causing, for large cluster sizes, a nondetectable fragmentation during the observation time window [15]. For our experimental conditions, and for a photon energy in the energy region subtended by surface plasmon absorption, i.e., 1 to 3 eV, single-photon-induced evaporation cannot be observed within the few microsecond time window for K_n^+ with $n > 100$.

In order to overcome this problem we performed a *multistep photon excitation.* The laser flux density is low enough so that the time interval between two successive absorptions is larger than the relaxation time. Moreover, for a given photon energy $h\nu$ the laser fluence range is chosen to induce evaporation *after* the 10-ns laser pulse duration but *before* the few microsecond observation time window. The rate equations for the multistep q photon absorption during the laser pulse

$$\begin{aligned} &K_n^+(E_0^*)+h\nu \rightarrow K_n^+(E_1^*) \\ &\quad\vdots \\ &K_n^+(E_k^*)+h\nu \rightarrow K_n^+(E_{k+1}^*) \\ &\quad\vdots \\ &K_n^+(E_{q-1}^*)+h\nu \rightarrow K_n^+(E_q^*) \end{aligned} \tag{1}$$

are

$$\begin{aligned} &\frac{dK_n^+}{dt}(E_0^*) = -\sigma\phi K_n^+(E_0^*) \\ &\quad\vdots \\ &\frac{dK_n^+}{dt}(E_k^*) = \sigma\phi K_n^+(E_{k-1}^*) - \sigma\phi K_n^+(E_k^*) \\ &\quad\vdots \\ &\frac{dK_n^+}{dt}(E_q^*) = \sigma\phi K_n^+(E_{q-1}^*) \end{aligned} \tag{2}$$

where $K_n^+(E_k^*)$ is the number of mass selected K_n^+ parents which have absorbed k photons during the laser pulse τ, ϕ is the photon flux density, and σ is the photo-

absorption cross section for a photon having an energy $h\nu$. σ is assumed to be little dependent of the cluster temperature.

The solution of these equations is a Poisson distribution. The number of clusters K_n^+ having internal energy E_k^* after absorbing k photons with $1 < k < q$ is

$$K_n^+(E_k^*) = K_n^+(E_0^*)(1/k!)(\sigma\phi\tau)^k \exp[-(\sigma\phi\tau)] . \quad (3)$$

During the few microsecond observation time window, the excited $K_n^+(E_k^*)$ clusters evaporate p atoms per cluster according to the energy balance

$$kh\nu = pD + E_f^* - E_0^* , \quad (4)$$

where E_0^* and E_f^* are the internal energies of the parent K_n^+ and the fragment K_{n-p}^+ entering and leaving the observation region, respectively. D is the mean value of the dissociating energy for clusters having between n and $n-p$ atoms [15]. Under these conditions the photofragment distribution reflects the excitation Poisson distribution, as shown in Fig. 1. Such a distribution peaks for

$$k_{max} = \sigma\phi\tau \quad (5)$$

which corresponds to a number of evaporated atoms

$$p_{max} = (E_0^* - E_f^*)/D + \sigma\phi\tau h\nu/D . \quad (6)$$

Considering the average laser power as variable

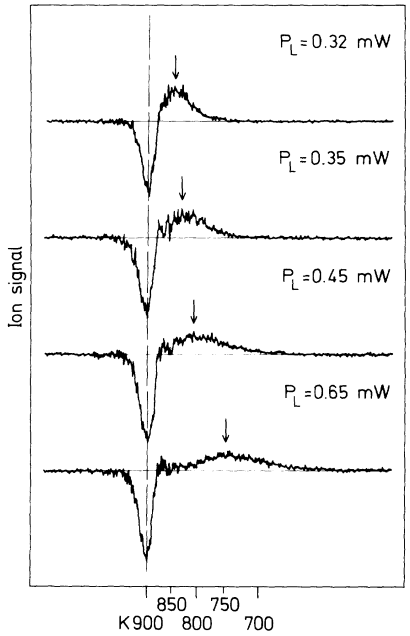

FIG. 1. Multistep photofragmentation data of K_{900}^+ obtained for several laser powers. The spectra recorded from the difference between the laser on and off clearly exhibit the depletion (negative dip) of K_{900}^+ parent ion which produces a Poisson distribution for the fragments. The dashed line marks the parent distribution. The arrows show the maxima of the Poisson distribution of fragments.

$$P_l = fh\nu\phi\tau\Sigma , \quad (7)$$

where Σ is the cross-sectional area of the laser beam and f is the frequency of the laser repetition rate, the number of evaporated atoms is

$$p_{max} = (E_0^* - E_f^*)/D + \sigma P_l/\Sigma f D . \quad (8)$$

As shown in Fig. 2, for a given photon energy, the number of lost atoms at the maximum of the fragment distribution varies linearly with the laser power as expected from Eq. (8). The slope of the straight line gives the absorption cross section. We note that this straight line does not pass through zero. The P_l axis intercept gives the number of photons which must be absorbed by the parent cluster before the first evaporation is observed [15]. This experimental procedure based on photoevaporation within a given time window of few microseconds only provides information about the photoabsorption of hot clusters. For alkali clusters with a few hundred atoms and binding energy of about 1 eV, statistical theories of evaporation [16,17], based on the number of evaporated atoms, suggest our cluster temperature during the photon absorption lies within the limits of 600 and 800 K.

Figure 3 shows the absorption cross sections for K_{500}^+ and K_{900}^+ versus the photon energy. The error bars of 25% result from the precision to determine the cross-sectional area Σ of the laser beam and the slope of the straight line of Fig. 2. Experimental data for each cluster are interpreted in terms of Mie theory [18]. For spherical metallic particles which are much smaller than the wavelength, the absorption cross section based on the Drude dielectric function is

$$\sigma_n(h\nu) = \sigma_n(h\nu_0)\frac{[h\nu\Gamma]^2}{[(h\nu)^2 - (h\nu_0)^2]^2 + [h\nu\Gamma]^2} , \quad (9)$$

where ν_0 is the Mie frequency, which is also known as the plasma frequency of a metallic sphere with n electrons,

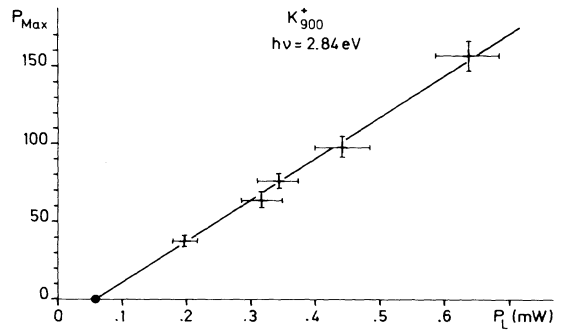

FIG. 2. Number of neutrals ejected at the maximum of the fragment distribution, from Fig. 1, is plotted vs the laser power average. Error bars indicate the precision with which the position of the maximum is determined from several runs of measurements as well as the precision for the laser power P_l.

and Γ the width of the resonance. The experimental data can be interpreted by using Eq. (9) with three fitting parameters, $\sigma_n(h\nu_0)$, $h\nu_0$, and Γ. Such a fit indicates that large potassium clusters are roughly spherical in agreement with theoretical predictions [19,20] which indicate that the deformation of large clusters is less pronounced than for small ones [21]. However, for large masses the cluster deformation can contribute to a broadening of the cross-section profile. The inherent temperature distribution produced by the experimental procedure also broadens the resonance profile.

The parameters used to fit the resonance are given in Table I together with those for small masses [2]. From the table we observe the resonance energy shift toward the blue as n increases. The shift of the resonance as a function of cluster size is of fundamental interest as a test for the validity of different models.

From the Drude model the plasma frequency of a metallic sphere is connected to its electronic density n_e [22] by the relation

$$h\nu_0 = \hbar(4\pi n_e e^2/3m)^{1/2}. \tag{10}$$

Assuming a metal cluster to be a metallic droplet with n electrons in a volume V its electronic density is $n_e = n/V$. In the simplest approximation $V = \frac{4}{3}\pi r_s^3 n$ where r_s is the Wigner-Seitz radius [22], the plasma frequency is

$$\nu_0 = \frac{1}{2\pi}\left(\frac{e^2}{mr_s^3}\right)^{1/2} = \frac{\nu_p}{\sqrt{3}}, \tag{11}$$

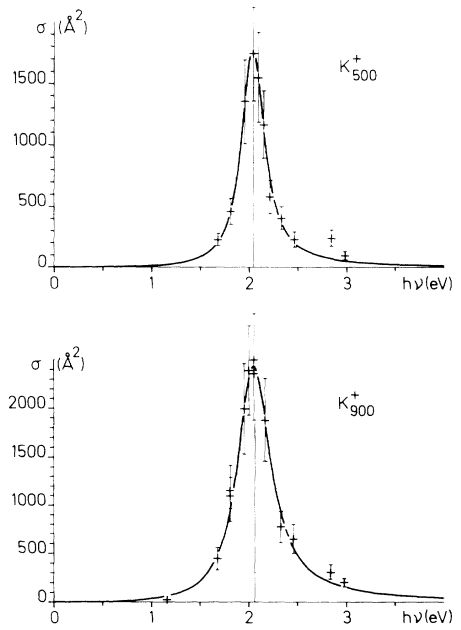

FIG. 3. Photoabsorption cross section profiles for large cluster ions K_{500}^+ and K_{900}^+ as a function of photon energy. The parent masses are distributed around the mean mass through the resolution of the selection (few masses).

TABLE I. Resonance energy $h\nu_0$, absorption cross section $\sigma(h\nu_0)$, and resonance width Γ, deduced from experimental absorption profiles, as a function of cluster size.

	$h\nu_0$ (eV)	$\sigma(h\nu_0)$ (Å²)	Γ (eV)
K_9^+	1.93	26	0.22
K_{21}^+	1.98	88	0.16
K_{500}^+	2.03	1750	0.28
K_{900}^+	2.05	2500	0.4

is independent of the cluster size, and is equal to the plasmon frequency of a spherical electron gas of radius r_s. In this model the bulk plasmon energy for potassium is $h\nu_p = 4.3$ eV and the Mie resonance energy $h\nu_{\text{Mie}} = 2.48$ eV. In order to interpret the observed blueshift as the cluster size increases, a more realistic volume of the delocalized electron gas must be taken into account. The size of the electron distribution in clusters is larger than is estimated on the basis of the volume per atom in the bulk [7,23]. The volume turns out to be significantly larger than the previous value and is given by

$$V = \tfrac{4}{3}\pi(r_s n^{1/3} + \delta)^3, \tag{12}$$

where δ is the electron spillout parameter [23].

The corresponding plasma frequency is then

$$\nu_0 = \frac{\nu_p}{\sqrt{3}}\left[1 + \frac{\delta}{r_s} n^{-1/3}\right]^{-3/2}, \tag{13}$$

which is proportional to $n^{-1/3}$ for large n.

Figure 4 is an illustration to show that quantitative agreement cannot be achieved between the classical model and the experimental data. We extended the calculation of the collective resonance frequency in singly charged spherical positive ions by using either the analytical approach formulated by Kresin [8] or the available program of Bertsch [12], which we have adapted for large masses. In all cases the calculated values are larger than the experimental ones. Figure 4(a) shows also the limit of the experimental value of the resonance energy when R is infinity: $h\nu_\infty$ deduced either from a recent measurement of surface plasmon energy $h\nu_{sp}$ [24], i.e., $h\nu_\infty = h\nu_{sp}\sqrt{2/3} = 2.24$ eV or from the bulk measurement [25] $h\nu_\infty = h\nu_p\sqrt{1/3} = 2.22$ eV. It is well known that the disagreement between the measured plasma frequency for the bulk and the value deduced from the Drude model is related to ionic core polarization and the effective mass of the electron [25]. In particular, for clusters the RPA calculation which treats positive ionic cores as a uniform positive background with radius $r_s n^{1/3}$ is not sufficient.

Figure 4(b) presents the behavior of the resonance energy divided by the limiting value when R is infinity versus $n^{-1/3}$ for the classical and RPA calculations as well as for the experiment. The experimental data con-

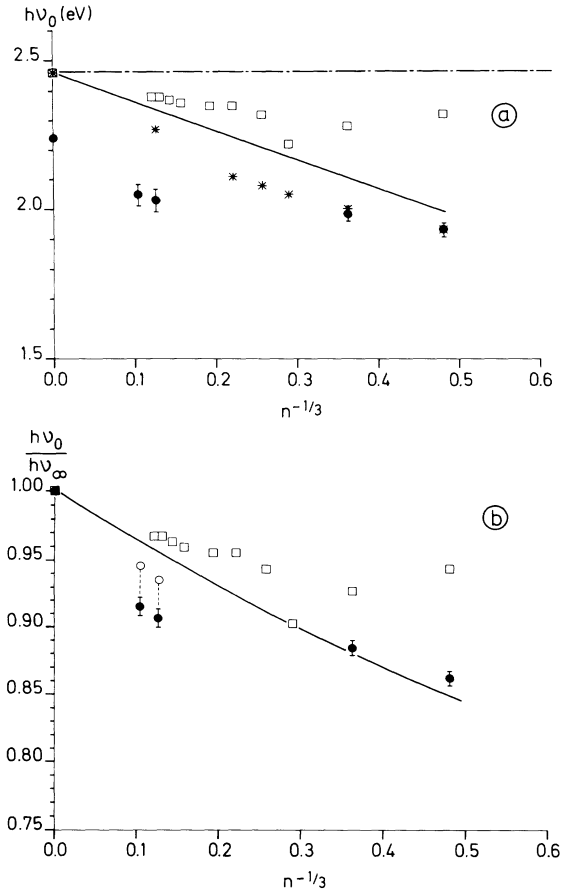

FIG. 4. (a) Resonance energy vs $n^{-1/3}$. The two straight lines are the classical value of the Mie resonance energy variations with spillout [23] (dash-dotted line) and without spillout (solid line). The asterisks and the squares are the calculated values from Refs. [8] and [12], respectively. The dots are our experimental data for clusters and the value deduced from a measurement of the surface plasmon resonance when n is infinity [24]. (b) The plasmon energy divided by the limiting value when n is infinity, $h\nu_0/h\nu_\infty$, vs cluster size for calculated and experimental values (see the text).

verge more slowly to the infinite limit than the calculated values. One reason may be due to the experimental conditions that caused larger clusters to have higher temperature. The temperature (700 K) of large clusters K_{500}^+ and K_{900}^+ is larger than the temperature (350 K) of small ones K_9^+ and K_{21}^+ [15]. An increase in temperature produces a cluster dilatation which induces a redshift in the plasmon frequency. A simple estimate gives a shift of 1% per 100 K [26]. From our experimental data the estimated values for the resonance energy that we could expect for K_{500}^+ and K_{900}^+ at 350 K are plotted (open circles) in Fig. 4(b), which still remain lower than calculated values.

The authors want to thank S. Björnholm for stimulating discussions concerning the temperature shift.

[1] W. de Heer, K. Selby, V. Kresin, J. Masui, M. Vollmer, A. Chatelain, and W. Knight, Phys. Rev. Lett. **59**, 1805 (1987).
[2] C. Bréchignac, Ph. Cahuzac, F. Carlier, and J. Leygnier, Chem. Phys. Lett. **164**, 433 (1989).
[3] C. Wang, S. Pollack, and M. Kappes, Chem. Phys. Lett. **166**, 26 (1990); J. Chem. Phys. **90**, 2496 (1991).
[4] H. Fallgreen and T. P. Martin, Chem. Phys. Lett. **168**, 233 (1990).
[5] J. Blanc, M. Broyer, J. Chevaleyre, Ph. Dugourd, H. Kühling, P. Labastie, M. Ubricht, J. P. Wolf, and L. Wöste, Z. Phys. D **19**, 7 (1991).
[6] J. H. Parks and S. McDonald, Phys. Rev. Lett. **62**, 2301 (1989).
[7] W. Eckardt, Phys. Rev. B **31**, 6360 (1985); W. Eckardt and Z. Penzar, Phys. Rev. B **43**, 1322 (1991).
[8] V. Kresin, Phys. Rev. B **39**, 3042 (1989); **40**, 12508 (1989).
[9] C. Yannouleas, R. A. Broglia, M. Brack, and P. F. Bortignon, Phys. Rev. Lett. **63**, 255 (1989).
[10] L. Serra, F. Garcia, M. Barranco, J. Navarro, C. Balbas, and A. Mañanes, Phys. Rev. B **39**, 8247 (1989).
[11] V. Bonacic-Koutecky, P. Fantucci, and J. Koutecky, J. Chem. Phys. **93**, 3802 (1990).
[12] G. Bertsch, Comput. Phys. Commun. **60**, 247 (1990).
[13] P. Fayet and L. Wöste, Z. Phys. D **3**, 177 (1986).
[14] M. L. Alexander, M. A. Johnson, N. E. Levinger, and W. C. Lineberger, Phys. Rev. Lett. **57**, 976 (1986).
[15] C. Bréchignac, Ph. Cahuzac, J. Leygnier, and J. Weiner, J. Chem. Phys. **90**, 1492 (1989); C. Bréchignac, Ph. Cahuzac, F. Carlier, M. de Frutos, and J. Leygnier, J. Chem. Phys. **93**, 7449 (1990).
[16] O. K. Rice and H. L. Rampsperger, J. Am. Chem. Soc. **49**, 1617 (1927).
[17] C. E. Klots, J. Chem. Phys. **83**, 5854 (1985).
[18] G. Mie, Ann. Phys. (Leipzig) **25**, 377 (1908).
[19] S. G. Nilsson, Mat. Fys. Medd. K. Dan. Vidensk. Selsk. **29**, 16 (1955).
[20] K. Clemenger, Phys. Rev. B **32**, 1359 (1985).
[21] C. Bréchignac, Ph. Cahuzac, F. Carlier, M. de Frutos, and J. Leygnier, Chem. Phys. Lett. **189**, 28 (1992).
[22] N. W. Ashcroft and N. D. Mermin, *Solid State Physics* (Holt, Rinehart and Winston, New York, 1976).
[23] E. Engel and J. Perdrew, Phys. Rev. B **43**, 1331 (1991).
[24] K. D. Tsuei, E. W. Plummer, and P. J. Feibelman, Phys. Rev. Lett. **63**, 2256 (1989).
[25] A. vom Felde, J. Spröser-Prou, and J. Fink, Phys. Rev. B **40**, 10181 (1989).
[26] *Hand Book of Chemistry and Physics* (Chemical Rubber, Cleveland, 1967), p. 56.